

MSEC_ICMP2008-72492

A Low Cost Wireless Tool Tip Vibration Sensor for Milling

Christopher A. Suprock

Department of Mechanical Engineering
University of New Hampshire
Durham, NH, USA
casuprock@suprocktech.com

Raed Z. Hassan

Department of Mechanical Engineering
University of New Hampshire
Durham, NH, USA
raed.hassan@unh.edu

Barry K. Fussell

Department of Mechanical Engineering
University of New Hampshire
Durham, NH, USA
barry.fussell@unh.edu

Robert B. Jerard

Department of Mechanical Engineering
University of New Hampshire
Durham, NH, USA
robert.jerard@unh.edu

ABSTRACT

A low cost, wireless vibration sensor system has been developed for noninvasive integration into commercial end milling tool holders. Electret based accelerometers are used as the sensors and a Bluetooth compatible digital transmitter is used as the sensor interface. The use of mass market consumer electronic components is low cost and plug and play with modern PC hardware. Two prototypes were built and, in both cases, were able to collect good quality data at high sampling rates. The objective of the research is to enable accurate observation of NC metal cutting system dynamics. Initial results indicate the system can be used to estimate tool runout and detect the onset of regenerative chatter, prior to workpiece damage.

INTRODUCTION

Wireless data transmission is starting to be widely used in industrial process control. For example, Callaway [1] discusses the application of wireless sensor networks for shop floor deployment. Wireless process control has numerous benefits including a low profile, ease of deployment, and the ability to monitor from a central location. Similarly, Sudararajan et. al [2] describe the potential of wireless monitoring specifically for machine tools.

Historically, the ability to record in-process data at an endmill tool tip has been limited by the sensor location. Often, these sensors are mounted on the material workpiece or the machine spindle at significant physical distance from the cutting process. Recently, Wright et. al [3] took advantage of wireless

transmission for measuring cutting tool temperature. In this work, resistive temperature detectors (RTDs) were placed on the backside of end-mill inserts. A primary goal of this research was to demonstrate the possibility for small form-factor wireless systems applied to tool condition monitoring. The success of this project is a promising exhibit of wireless applicability to endmill tool condition monitoring.

Endmill vibration data contains a broad spectrum of useful information but requires significantly higher bandwidth than temperature measurement. In an example by Dini et. al [4], close proximity wireless acquisition of cutting torque signals was conducted using a commercial rotating dynamometer. In this case, the dynamometer is directly placed between the spindle and tool. This method is excellent for capturing a torque signal, however, commercial dynamometers are high in cost and increase the spindle compliance.

Vibration measured by spindle mounted sensors suffers from attenuation and noise introduced by spindle bearings, tool holder, and collet interfaces. Accurate measurement of in-process tool tip response is vital to the development of tool dynamic models. Cheng et al. [5], used receptance coupling substructure analysis (RCSA) to indirectly characterize tool tip dynamics during spindle rotation. Although informative, these techniques require precision tool holding setups. Like any indirect estimation method, RCSA is not as effective as measuring the signal at its source.

By employing wireless techniques and embedded sensors, the tool-workpiece interactions can be more clearly observed. It should be possible to monitor the stability of the

cut during changing cutting conditions and therefore improve cutting efficiency by avoiding chatter or forced vibrations. The sensor may also be useful for detecting undesirable tool eccentricity, i.e. runout. Moreover, it is possible to monitor these items on multiple machines from a control location without interfering with shop floor activity. This paper will describe the design and fabrication of two prototypes. Vibration sensor data was collected during a number of cutting tests.

BACKGROUND

To better understand dynamic end milling problems such as tool chatter, wear, and run out, it is helpful to observe the tool tip response characteristics directly during the cutting process. The system is designed to transmit acceleration data directly from an end mill tool tip or from individual cutting inserts. This capability is critical to advance physical modeling and condition monitoring techniques for metal cutting.

Wireless Data Transmission and Acquisition Method

In an endmilling system, significant challenges to wireless bandwidth may exist from motor noise. During the machining process, spindle and bed motors generate a wide and continually changing spectrum of interference. This fact increases the difficulty of wireless transmission with fixed frequency or amplitude methods. The problem can be approached in two ways: Characterizing the spectrum of motor noise and designing a transmitter to avoid it for a particular milling process, or, employing an active noise avoidance scheme such as frequency hopping spread spectrum (FHSS). Because of the multitude of mill configurations and processes, it is desirable to choose the second technique, since it is most amicable to generalization.

Since 1998, FHSS techniques have been commercially standardized for use on the license-free ISM band (2.4-2.4835 GHz). This standardization has been motivated by attention from the communications hardware industry, with one particular standard being defined through the Bluetooth Special Interest Group [6]. High quality audio transmission has been at the forefront of this technology with interoperability between all Bluetooth audio devices being based on the Audio Distribution Model [7]. Transmission bandwidth requirements conform to mandatory sampling requirements of 44.1 and 48.0 kHz. These rates are enforced for the benefit of the transmitter by the receiver device [7].

For this work, a commercially available 16 bit audio transmitter is used. The transmitter circuit is modified from a Jabra BT350 personal microphone headset (retail cost approximately \$20). This transmitter contains the necessary transceiver hardware in addition to a signal conditioning circuit for an impedance sensor load. Specifically, this transmitter is designed to transmit data from an electret condenser microphone or similar impedance-changing input sensor. For instance, this circuit could also be utilized to transmit an impedance signal from a strain gage setup. This transmitter conforms to the published specifications in [7] and is capable of sending an audio signal to the Bluetooth receiver at 48.0 kHz. However, the analog signal conditioning circuit on this

particular transmitter has a high frequency rolloff with a corner frequency of 3250 Hz. This is observed in preliminary testing of the device and exists to prevent aliasing in the A/D. The effective frequency bandwidth of this transmitter is approximately 100 to 3500 Hz. This is sufficient for observing many common milling phenomena.

Using an Electret Condenser as an Accelerometer

An electret condenser module responds to vibration input by changing its impedance. The impedance of a FET changes in linear (drain) mode according to the proximity of the electret diaphragm to a stationary backplate. The electret used for this study is a Hosiden # KUB2823 and is characteristic of a commercially available electret condenser (approximate retail cost \$0.50). This particular electret employs a diaphragm and is similar to the design detailed in [8].

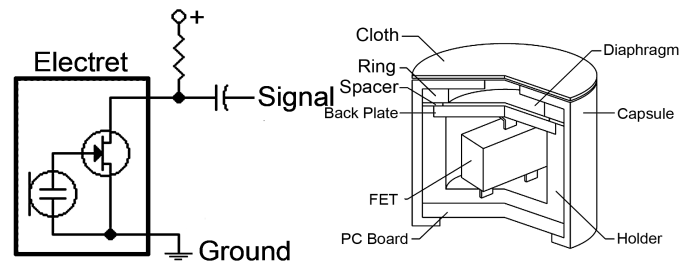


FIGURE 1. ELECTRET CONDENSER MODULE [14]

It is important to confirm that the electret condenser is capable of producing a repeatable linear response. The electret condenser specifications assume operation in air, where the diaphragm responds directly to changes in air pressure caused by sound waves. However, when implemented as an accelerometer, the dynamics of this sensor are significantly altered from the manufacturer's intended specification and must be reevaluated.

To accomplish this, a sinusoidal vibration input is generated using a shaker table. A single-axis PCB piezoelectric accelerometer (Model 320 C33, serial number 5901) is fixed to the table at the same reference point as the electret sensor. The output sensitivity of this accelerometer is 100mV/g with a maximum range of 50 g's. The piezoelectric accelerometer is amplified through a PCB charge amplifier. Both the piezoelectric accelerometer and the electret sensor signals are sampled at 20 kHz. Figure 2 shows the shaker table and attached sensors and corresponding DUT block diagram.

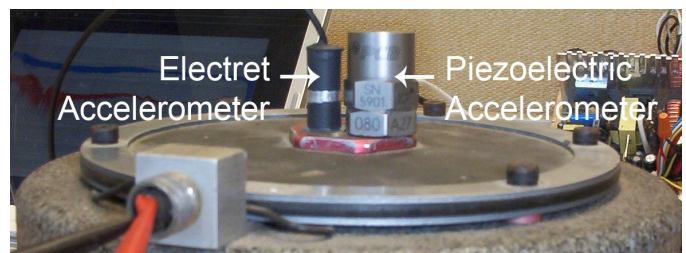


FIGURE 2. SENSORS MOUNTED ON SHAKER

The PCB accelerometer has a known flat frequency response from 1 Hz up to 4 kHz and provides the baseline from which the electret sensor is benchmarked. Figure 3 presents the results of these experiments, with Figure 3A showing the spectra of both piezoelectric and electret accelerometers and Figure 3B showing the linear gain relationship present at three discrete frequencies.

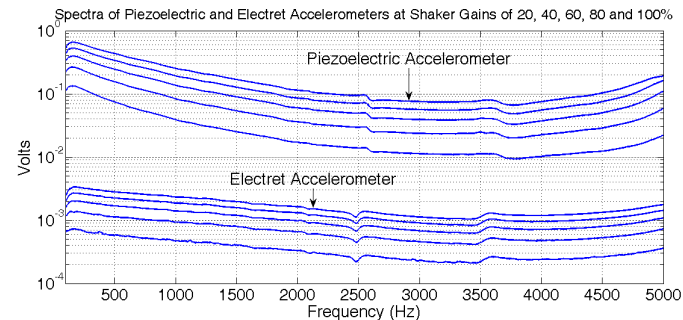


FIGURE 3A. LINEAR RESPONSE OF THE ELECTRET ACCELEROMETER

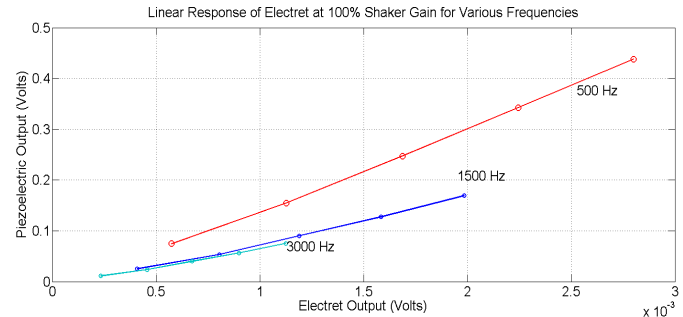


FIGURE 3B. LINEAR RESPONSE OF THE ELECTRET ACCELEROMETER

As a result of the linear response, a basic transfer function, R , between the electret and flat (piezoelectric) response can be given as:

$$R(\omega) = \frac{P(\omega)}{E(\omega)} \quad (1)$$

Where P and E are the piezoelectric and electret response spectra respectively. Robustness testing and further exploration of this sensor calibration technique for an electret accelerometer is documented in [9].

For a video describing the electret accelerometer testing described in this section, refer to refer to [13].

PROTOTYPE #1: DESIGN AND FABRICATION

The process of embedding a sensor at the tool tip required solutions to a variety of design challenges.

Design constraints for the sensor system include:

- No intrusion in the machining envelope
- No interference with automatic tool change

- Minimal cost
- Must operate in the presence of coolant
- Must maintain rotational balance
- No effect on tool compliance

Two prototypes were designed, built and tested. The first prototype consists of a 76.2 mm (3”) OD four insert facemilling tool holder. This platform was chosen for a first prototype since it provides sufficient room for sensor and transmitter placement without interfering with the cutting process. The location for noninvasive sensor deployment is a fatigue notch located behind/below the insert set bolt. Figure 4A details the location of the tool holder within the mill. Placement of the electret sensor is within 8 millimeters of the tool-workpiece interface. The sensor system has been integrated in a way that does not impact the structural integrity of the tool holder. As a result, only a slight modification is required for sensor embedding. Figure 4B shows a closeup view of the insert tool holder, before modification.

Placement of a sensor behind each insert cutter provides vibration input from each individual insert as it enters and exits the workpiece. Recalling that the sensors used in this device are linear impedance changing, the sensors are wired in series. Because the sensors are wired in series, the sensor system will be more sensitive to vibrations in the tangential direction and should be relatively insensitive to vibrations in the X and Y direction. Figure 5 details the orientation and location of the accelerometers.

Placement of the transmitter circuit and sensor wiring is facilitated by a shroud designed to mount onto the tool holder body. This shroud is fabricated from ABS plastic on a rapid prototyping machine. The shroud provides wire routes for the sensors in addition to protection from chips and cutting fluid. Figure 6 provides detail on the mounting of this shroud in both use-ready and charging modes. The transmitter is powered by a rechargeable 3.7V lithium ion battery, also mounted within the protective shroud. The battery is a component in the transmitter assembly and is provided with the retail transmitter. For a video of fabricating the tool holder described in this section, refer to [13].

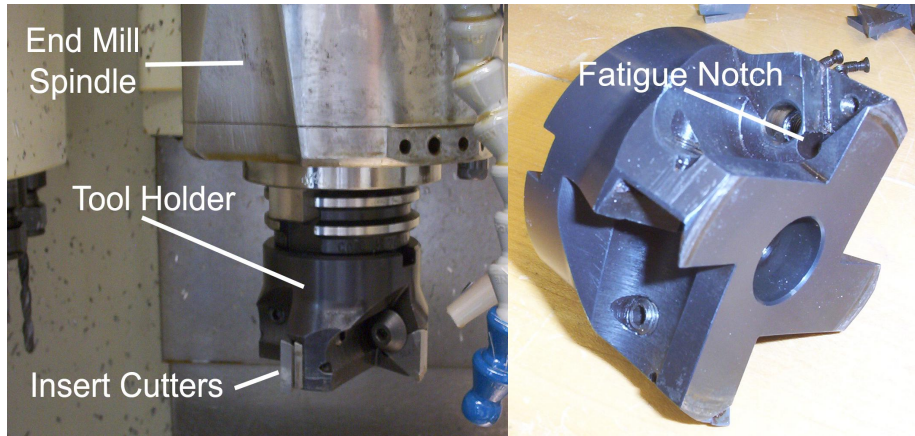


FIGURE 4A & 4B. SPINDLE AND SENSOR LOCATION

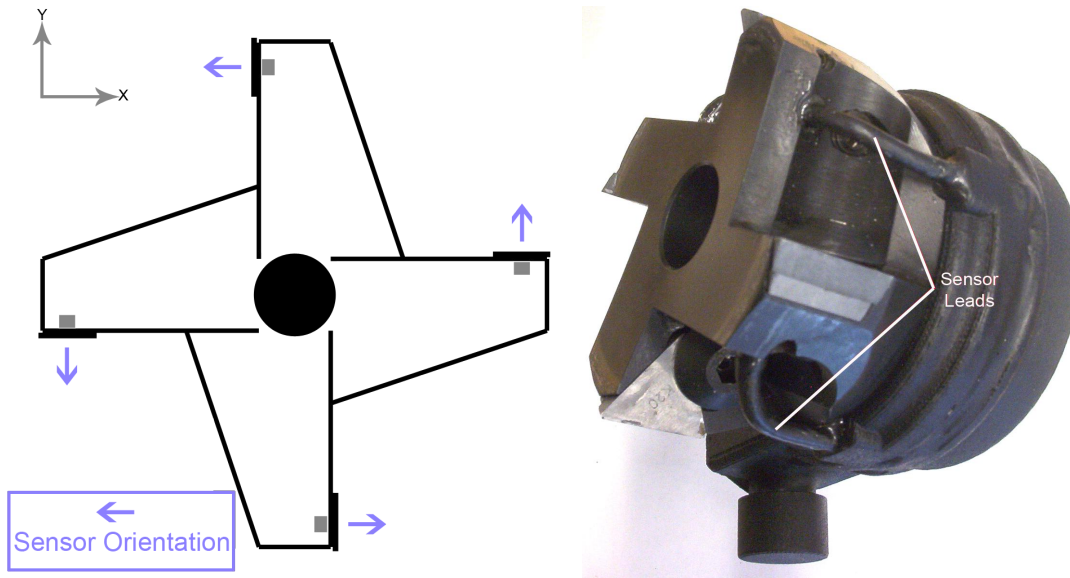


FIGURE 5. SENSOR ORIENTATION

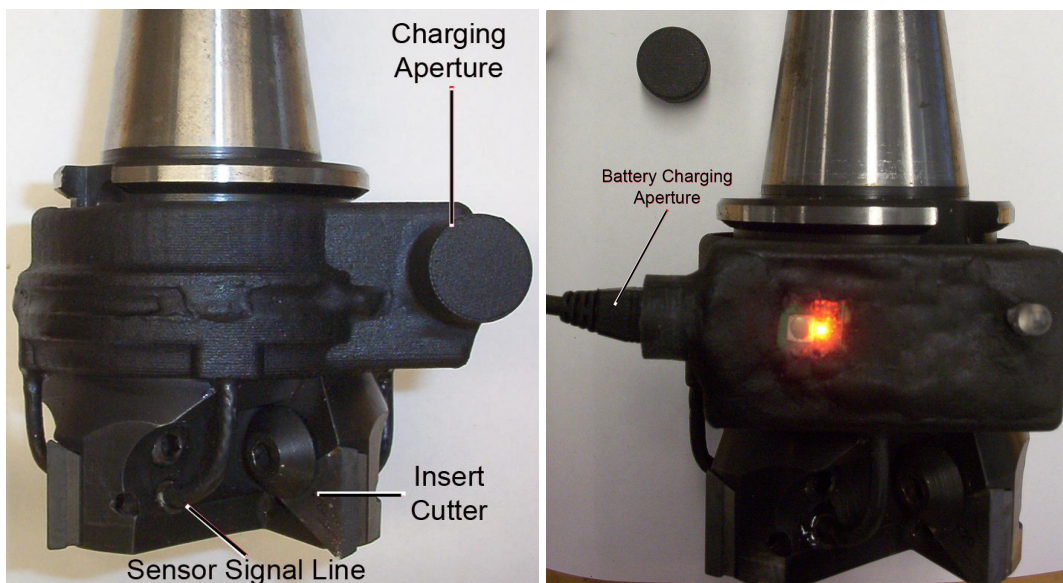


FIGURE 6. TRANSMITTER AND WIRING SHROUD

TESTING PROTOTYPE #1

Cutting tests were performed to evaluate the performance of the device. The tests performed were 75% immersion (57.15 mm radial immersion) linear upmill cuts through 6061 aluminum. The spindle speed for these tests was 800 RPM with a 2.54 mm axial depth and feed rate of 0.762 m/min. The cut length was 152.4 mm between workpiece entrance and exit. The output from the transmitter was recorded with a data acquisition PC sampling at 20 kHz.

A plot of the recorded data is shown in Figure 7. The noise floor was very low, indicating that the transmitter effectively avoided motor noise and delivering an uninterrupted signal during the test. The low level of noise can be seen in Figure 7 before and after the cutting starts.

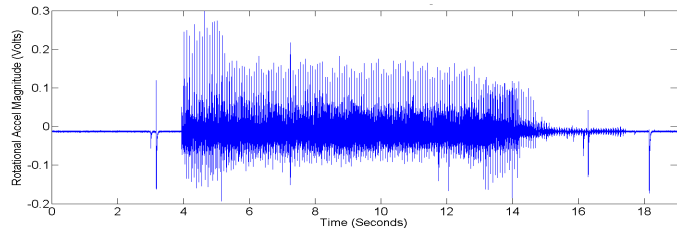


Figure 7. Time Signal From the Four Insert Tool Holder Test

Entrance and exit effects are clear, with higher magnitudes occurring during workpiece penetration (at 4 to 5 seconds) and decaying magnitudes as the tool exits the material (at 14 to 15 seconds). Signal spikes are observed at 2.6 and 18.2 seconds, corresponding to the instant at which the bed started and stopped. The detection of bed movement is a curious development. Recalling that the orientation of the sensors was intended to cancel X and Y components of acceleration. Since the tool only moves in the Z direction we are not measuring acceleration of the tool but it must either be an electrical artifact or vibration transmitted from the bed to the tool via the machine structure. Further investigation is warranted.

Sensor data for three revolution of the tool is shown in Figure 8. The toothpass frequency of 53.33 Hz is apparent in the time data with a period of 0.0187 seconds between inserts.

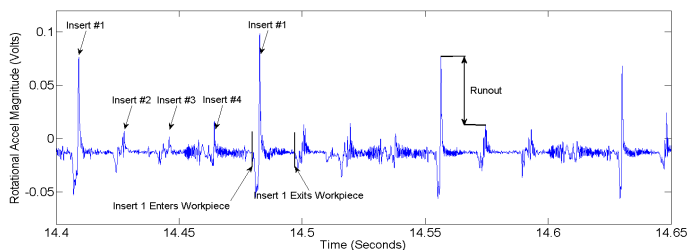


Figure 8. Details of The Time Signal

It is apparent that runout is present, with insert 1 producing a significantly larger vibration magnitude than inserts 2 through 4. The presence of runout was confirmed by physical measurement with a dial indicator showing a 0.23 mm

difference between the high and low measurements. The recorded data correctly reflects the underlying physics. This is admittedly a rather large runout, but in fact it was unplanned and we were unaware of the presence of runout until we looked at the data. This amount of runout would clearly have a negative affect on part accuracy and surface finish. We conjecture that the sensor would do an equally good job of detecting a broken tooth.

The sensor signal is further expanded in Figure 9 which shows the cutting action during the time when a single insert is in contact with the workpiece.

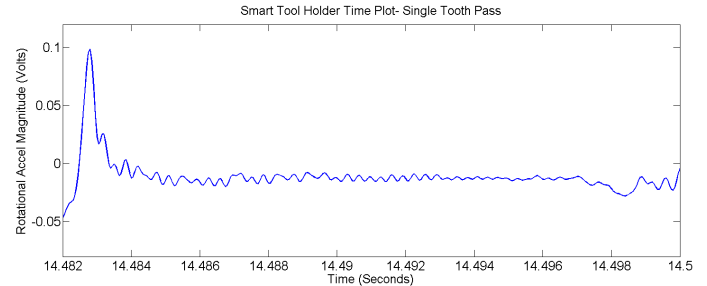


Figure 9. Single Insert Cutter Toothpass

For a movie showing tests of Prototype #1, visit the UNH DML website [13].

PROTOTYPE #2: DESIGN AND FABRICATION

The form factor of many tools does not permit placing sensors behind the teeth. We therefore made a prototype with a single sensor embedded in the center as illustrated in Figure 10. Embedding a sensor at the tool tip requires the solution of a variety of problems. First, the location of a sensor at the tool tip necessitates the use of coolant to prevent elevated temperatures and sensor malfunction. The use of coolant forces the electronic components of the system to be entirely insulated from the environment. A system was devised to generalize the use of interchangeable tool-sensor systems using the same tool holder/transmitter unit. This is a practical constraint considering the eventual market potential of the concept.

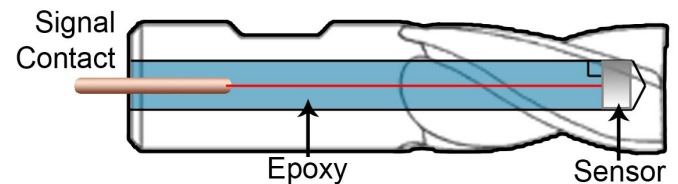


Figure 10. Model of a Tool Tip Sensor

For the second prototype, a Sandvik 19.05 mm diameter helical insert tool (RA390-019M19-11L Coromill 390) was selected. A helical insert tool was chosen since it is possible to embed the sensor and reuse the sensor integrated tool indefinitely, replacing failed inserts. The tool was modified with a 6mm axial hole for sensor placement and the sensor was embedded 5mm from the carbide cutting inserts. As shown in Figure 10, the sensor is oriented in the axial direction. Figure 11

presents a photograph of the sensor integrated tool with carbide cutters and sensor signal contact. An RCA type terminal contact was selected because it is axisymmetric and can easily mate with a counterpart terminal located in the tool holder.



Figure 11. 0.75" Helical Insert Tool

Although a 19.05 mm (0.75") insert tool was selected for this study, this design can accommodate any sensor integrated tool with a 19.05 mm shank. Designing the tool and tool holder as complimentary devices provides a system that is more resource-efficient and scalable than embedding sensors behind individual facemill inserts. The ability to reconfigure the tool holder with any variety of sensor integrated tools increases convenience for both research and potential production purposes.



Figure 12. Sensor Integrated Endmilling Tool Fixtured In a Transmitting Tool Holder

TESTING PROTOTYPE #2

Evolution of a tool tip sensor design enabled further opportunity to test the concept and observe the output for physical significance. To achieve this, a variety of tests were conducted to observe changes in output with respect to different cutting geometries. Table 1 details the geometries of the tests conducted.

Table 1. Test Cut Geometries

| Milling type | Slot | Down | Up | Down | Up | Down | Up |
|---------------------------------------|------|------|-----|------|-----|------|-----|
| Radial Immersion | Full | 75% | 75% | 50% | 50% | 25% | 25% |
| Geometry of Immersion (Cross Section) | | | | | | | |

All of these tests were operated at a constant spindle speed of 3819 RPM, axial depth of 5.08 mm, and followed a linear path in 6061 T6 Aluminum. The material removal rate was varied by changing the feed rates during each cutting

geometry test. These feed rates were calculated to maintain a uniform average chip thickness for different cutting geometries. The three thicknesses were selected to cover a range of chip loads (0.0127, 0.0508, and 0.127 mm). Table 2 provides the three feed rates used during each cutting geometry test.

Table 2. Test Cut Feed Rates

| | Slot | 75% Down | 50% Down | 25% Down | 75% Up | 50% Up | 25% Up |
|-----------------|-------|----------|----------|----------|--------|--------|--------|
| Feed 1 (in/min) | 6.0 | 5.33 | 6.0 | 8.0 | 5.33 | 6.0 | 8.0 |
| Feed 2 (in/min) | 24.0 | 21.33 | 24.0 | 31.99 | 21.33 | 24.0 | 31.99 |
| Feed 3 (in/min) | 59.99 | 53.32 | 59.99 | 79.99 | 53.32 | 59.99 | 79.99 |

During this test, we compared upmilling and downmilling cuts. While testing, it was noticeable that upmilling caused higher vibration magnitudes in the data. As expected, this seen in the average vibration magnitudes of Table 3. The upmilling cuts are observed to have a higher absolute magnitude for all tests. The difference in vibration magnitude between upmilling and downmilling cuts is significant and Figure 13 visually highlights the differences in magnitude.

Table 3. Vibration Magnitudes for Each Cut

| | Slot | 75% Down | 50% Down | 25% Down | 75% Up | 50% Up | 25% Up |
|----------------|--------|----------|----------|----------|--------|--------|--------|
| Feed 1 (Volts) | 0.0186 | 0.0146 | 0.0135 | 0.0134 | 0.0191 | 0.0191 | 0.0159 |
| Feed 2 (Volts) | 0.0581 | 0.0443 | 0.0417 | 0.0412 | 0.0519 | 0.0527 | 0.0459 |
| Feed 3 (Volts) | 0.1218 | 0.0946 | 0.0806 | 0.0808 | 0.1034 | 0.1016 | 0.0874 |

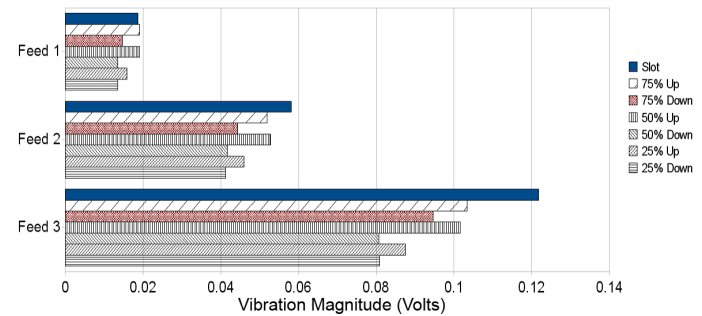


Figure 13. Vibration Magnitudes for Each Cut

Over the three feed rates tested, a linear relationship was found between the vibration magnitudes and the average chip thickness. The half immersion up and down milling cuts appear in the center of the set, shown in Figure 14. Since the half immersion trends are in the center of the spread, they are closest to the average slope and average intercept of the set. This observation is in agreement with [10], where half immersion tests were found to be preferable for force model calibration. However, unlike force or power, observing the relationship between chip thickness and vibration magnitude is relative to the spindle speed for these particular tests.

For a movie showing testing of Prototype #2, visit the UNH DML website [13].

OBSERVATION OF TOOL CHATTER

Finally, we designed a test to induce regenerative chatter during a slot cut. Similar to the other geometry tests, this cut is made in 6061 T6 aluminum at a spindle speed of 3819 RPM. However, unlike these tests, the axial depth of cut is increased to 10.16 mm (0.4") in order to induce chatter. The feed rate is set to 0.762 m/minute and the spindle speed is 3819 RPM.

Figure 17 shows the time response of the sensor during the development of chatter conditions. As expected, the vibration magnitude greatly increases as the chatter builds up. After the chatter condition accelerates and workpiece damage begins, the sensor output reaches saturation.

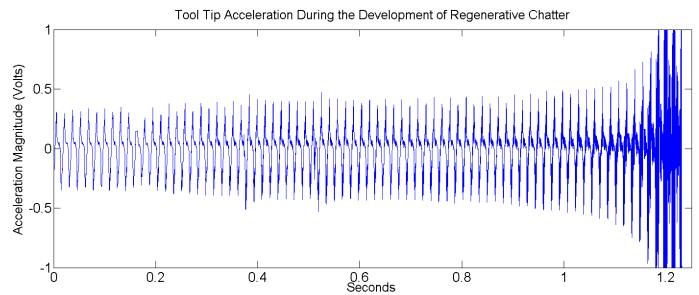


Figure 17. Development of Regenerative Chatter

Figure 18 provides a visual interpretation of how the regenerative chatter begins, showing a photograph of the slot cut accompanied by three acceleration frequency spectra. These three acceleration spectra are generated from the Figure 17 time data and are time-correlated to each segment of the slot cut photograph.

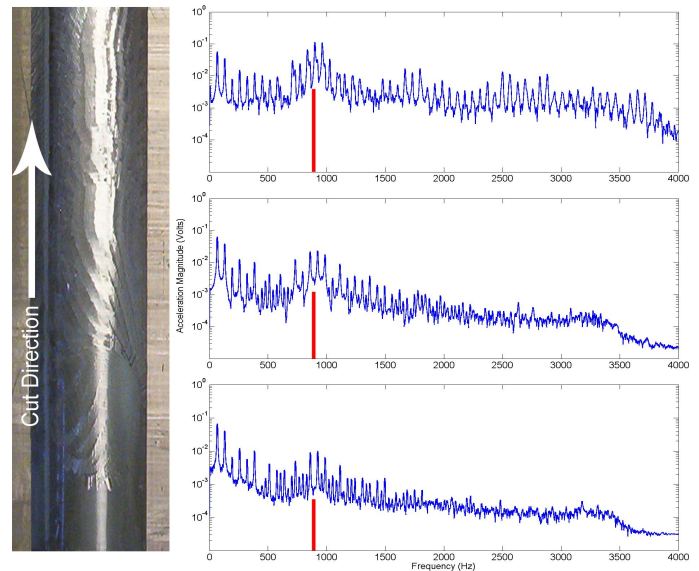


Figure 18. Slot Cut Photograph and Acceleration Frequency Spectra

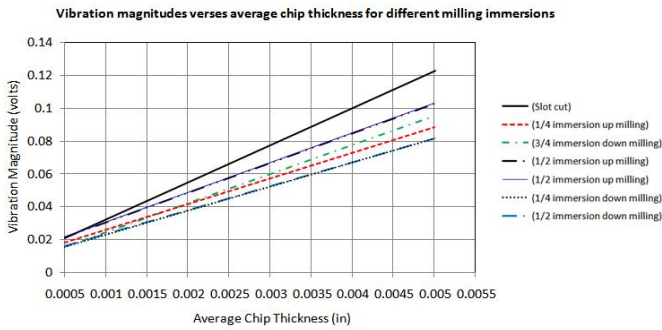


Figure 14. Vibration Magnitude vs. Chip Thickness

Another interesting observation of these tests is that the upmilling cuts exhibit a positive acceleration bias whereas the downmilling tests exhibit a negative acceleration bias. Intuitively, this makes sense due to the axial orientation of the sensor in the tooling unit. Because the electret diaphragm responds to acceleration and the insert tool holder is helical, cutting entrance during the downmill pulls the tool downward in the Z axis at a higher rate, causing a negative bias in the sensor. Although this bias exists between upmilling and downmilling operations, the absolute magnitude of the signals is unaltered. This result is encouraging since it enables distinction between upmilling and downmilling from the data, while the absolute magnitude of the signal is preserved. Figure 15 shows a time plot of both half immersion upmill and downmill cuts.

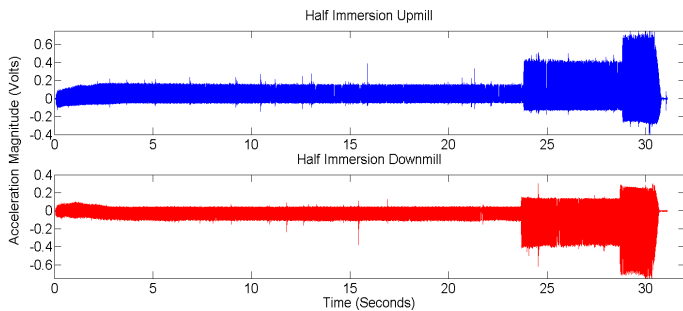


Figure 15. Half Immersion Upmill and Downmill Cuts

Figure 16 shows a plot of the data for a slot cut at the three feed rates shown in Table 2. In contrast to the upmilling and downmilling cuts, the slot cut exhibits a zero centered trend. This result makes since the slot cut is analogous to a simultaneous half immersion up and down milling operation.

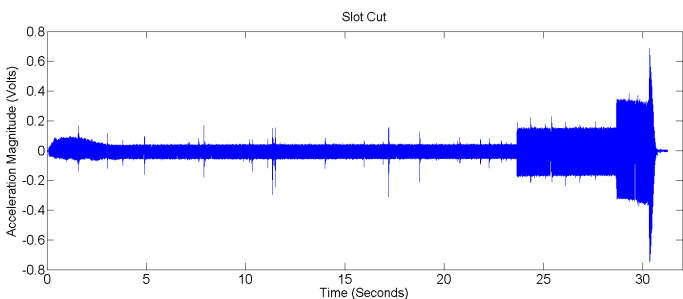


Figure 16. Slot Cut

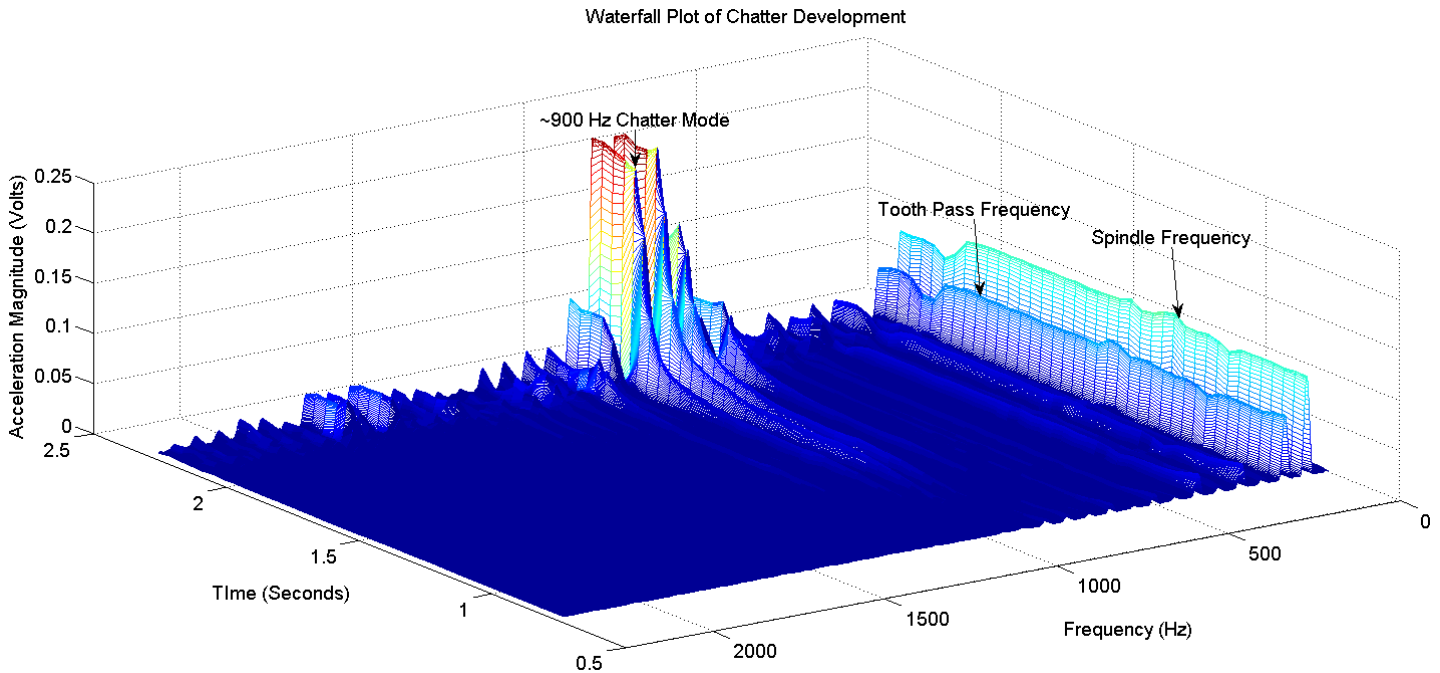


Figure 19 Waterfall plot of frequency content versus time.

The evolution of a chatter mode can also be observed in Figure 19 as a waterfall plot of frequency content over time. It is evident that the development of the chatter condition occurs over a 1.2 second period, with rapid acceleration towards the onset of workpiece damage. However, during the early development period, the surface finish remains normal. Therefore, by tracking elevations in the chatter mode, it may be possible to predict the onset of workpiece damage before it occurs.

PREDICTING STABLE SPINDLE SPEEDS

Although observing the early onset of chatter is suitable for an in-process safety measure, relying on this capability does not help with process planning. Ideally, cutting engagements and speeds would be chosen with prior knowledge of unstable conditions. In this way, process efficiency can be increased in an intelligent manner.

Traditionally, stability lobes are calculated from the Frequency Response Function (FRF) of the end mill spindle [15]. Unfortunately, current methods to generate the FRF do not include the effects of workpiece dynamics that occur during cutting. Since these effects are highly variable and difficult to directly measure, a method is designed for in-cut stability estimation using the sensor integrated tool.

To evaluate stable spindle speeds, a test is planned to continually vary spindle frequency over the duration of a single 114.3 mm slot cut. The range of spindle speeds chosen was from 2500 to 7375 RPM. The spindle speed is linearly increased over the length of the slot cut after the tool is fully immersed. The feed per tooth is maintained at 0.0254 mm by changing the feed rate as proportionally to spindle speed. The tool toothpass frequency varied from 83.33 to 245.83 Hz, providing input excitation at these frequencies. This test is

conducted both as described and by reversing the frequency sweep (from 7375 down to 2500 RPM). Figures 20 and 21 show the results of the forward and backward frequency sweep. Interesting results were obtained from these tests. The onset of instability is apparent in the time data by the presence of elevated magnitudes in the vibration signal.

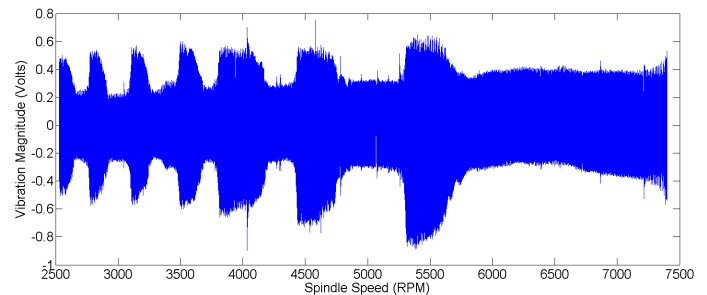


Figure 20. Increasing Spindle Speed, with Unstable Modes

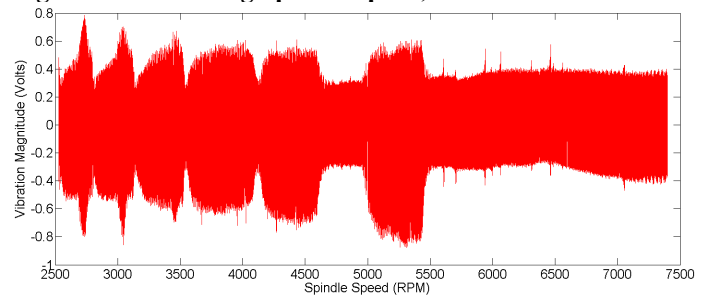


Figure 21. Decreasing Spindle Speed, with Unstable Modes

It is notable that the location of the unstable regions is shifted depending on whether the spindle speed is increasing or decreasing. Since regenerative chatter results from a surface finish phase difference, this effect has been coined “phase hysteresis”- the persistence of chatter into stable modes due to the decay of the residual surface waviness from the prior

instability. Although phase hysteresis occurs during the decay of instability, it can also be observed that the onset of chatter is sharply defined for both increasing and decreasing spindle speeds. These onset points identify the upper and lower bounds of the unstable modes. Because the test was conducted for both increasing and decreasing spindle speeds, the upper and lower boundaries of the unstable modes are clearly defined, regardless of phase hysteresis. To test this hypothesis, stable and unstable spindle speeds were chosen based on the two tests. Figure 22 shows the absolute vibration magnitudes from both tests superimposed for clarity. Vertical lines indicate the predicted stable spindle speeds chosen for verification.

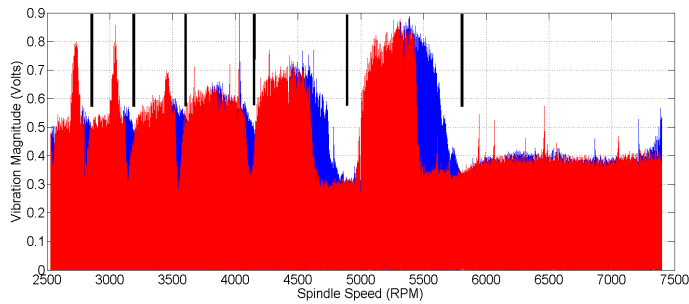


Figure 22. Superimposed Absolute Vibration Magnitudes from the Frequency Sweep Tests.

The speeds selected from Figure 22 are given in Table 4, as stable and unstable conditions.

Table 4. Predicted Stable and Unstable Spindle Speeds

| | | | | | | |
|----------------|------|------|------|------|------|------|
| Stable (RPM) | 2867 | 3197 | 3616 | 4153 | 4891 | 5808 |
| Unstable (RPM) | 2748 | 3063 | 3485 | 3850 | 4758 | 5340 |

Maintaining the same axial depth and 0.0254 mm feed per tooth, the spindle speeds in Table 4 were evaluated. For all six stable conditions predicted, the cuts were without chatter. For all six unstable conditions predicted, chatter was encountered. These tests were repeated three times with identical results.

These tests indicate that it is practical to predict stable spindle speeds using the sensor integrated tool. With a constant chip thickness, the material removal rate between the lowest and highest stable cutting condition was doubled. It is noted that this test did not disclose the safe and unsafe axial depths of cut, however, by repeating this experiment at several depths of cut, a complete experimental stability lobe diagram can be generated.

CONCLUSIONS AND FUTURE WORK

The development and testing of a sensor integrated wireless tool holder creates opportunities to better study the dynamics of metal cutting. This sensor was successfully used to learn more about complicated interactions at the tool-workpiece interface, specifically interactions affecting stability during cutting. The potential of this device for use in wear monitoring and dynamic force modeling is a promising area of future research.

For stability evaluation and chatter analysis, the tool holder system has shown promising results for monitoring stability during the cutting process. The device was successfully used to increase the productivity of material removal by finding higher stable speeds.

The wireless interface for this device was successful and shows that the Bluetooth or other FHSS standards are applicable to a machining environment where motor noise could disrupt many wireless techniques.

The ultimate goal for this device is a product capable of delivering powerful condition monitoring to industry without the need for a wired interface, at a low cost. However, this requires the development of knowledge and models capable of interpreting the collected data. Finally, the ability to observe the onset of regenerative chatter before surface damage occurs creates opportunities for increased industrial process efficiency and safety.

ACKNOWLEDGMENTS

The support of the National Science Foundation under grants DMI-0322869 and DMI-0620996 is gratefully acknowledged. We would also like to thank Mr. Peter Samuelson, Sandvik Application Specialist, for the donation of tooling and materials.

REFERENCES

- [1] Callaway, E.H. (2004), "Wireless Sensor Networks: Architectures and Protocols" CRC Press, September 2003 ISBN-13: 9780849318238
- [2] Sudararajan, V., Redfern, A., Schneider, M. and Wright, P. (2005) 'Wireless sensor networks for machinery monitoring', ASME International Mechanical Engineering Congress and Exposition, Orlando, Florida, USA.
- [3] Wright, P. K., Dornfeld, D. A., Hillaire, R. G., and Ota, N. K. (2006), "A Wireless Sensor for Tool Temperature Measurement and its Integration within a Manufacturing System", Trans. North American Manufacturing Research Institute, 2006, vol. 34
- [4] Dini, G., and Tognazzi, F. (2006), "Tool condition monitoring in end milling using a torque-based sensorized toolholder", Proceedings of IMechE: J. Engineering Manufacture, Vol. 221 Part B, pp 11-23 DOI:10.1243/09544054JEM559
- [5] Cheng, C.H., Schmitz, T.L., Duncan, G.S. (2007), "ROTATING TOOL POINT FREQUENCY RESPONSE PREDICTION USING RCSA", Machining Science and Technology, Vol. 11, Issue 3, July 2007, pp 433-446
- [6] Bluetooth Special Interest Group www.bluetooth.org

- [7] Bluetooth Special Interest Group (2007) "Advanced Audio Distribution Profile Specification" Revision 12. Document A2DP_SPEC. April 2007
- [8] Sessler, G.M. and J.E. West (1966). "Foil-Electret Microphones." *The Journal of the Acoustical Society of America*, Vol. 40, Issue 6, pp. 1433-1440.
- [9] Suprock, C.A., Fussell, B.K., Roth, J.T. (2008) "A Cost Effective Accelerometer and DAQ for Machine Condition Monitoring: A Feasibility Study." *Transactions of the North American Manufacturing Research Institution of SME*, Vol. 36
- [10] Xu, M., Jerard, R.B., and Fussell, B.K., (2007) "Energy Based Cutting Force Model Calibration for Milling" *Computer aided design and applications* Vol 4, Nos. 1-4, 2007 pp 341-351.
- [11] Suprock, C.A., Roth, J.T., Downey, L.M., (2007) "Failure Forecasting for Flat, Ball-Nose, Roughing, and Tapered Endmills Using Acceleration Data" *Transactions of the North American Manufacturing Research Institution of SME*, Vol. 35
- [12] Suprock, C.A. (2008) "Wireless Sensor Integrated Smart Tool Holder and Tooling for Metal Cutting" United States Patent and Trademark Office, Provisional Patent Application No. 61037033.
- [13] University of New Hampshire, Design and Manufacturing Lab, <http://unh.edu/dml>
- [14] Hosiden Online Electret Microphone Catalog
http://www.hosiden.co.jp/web/english/web/products/pdf/e_on06_mic.pdf
- [15] Altintas, Y. (2000) "Manufacturing Automation" Cambridge University Press, New York. ISBN: 0-521-65029-1